ARTICLE NO. 78-403

Effect of Thin Film Heat Transfer on Meniscus Profile and Capillary Pressure

P. C. Wayner Jr.*
Rensselaer Polytechnic Institute, Troy, N.Y.

Viscous flow in a thin film in the immediate vicinity of the interline (junction of solid-liquid-vapor) significantly affects the complete profile of an evaporating meniscus. An analysis based on the premise that fluid flow results from the London-van der Waals dispersion force is used to evaluate this change as a function of heat flux. The useful capillary pressure of the meniscus is significantly reduced as the interline heat flux is increased. The dispersion model predicts measurable changes in the meniscus heat-transfer characteristics which are related to the macroscopic optical properties of the solid and liquid.

Nomenclature

$\bar{A}$ = dispersion constant, J
G = constant in Eq. (10), m^{-2}
h = heat-transfer coefficient, $W \cdot m^{-2} \cdot K^{-1}$
h_{fg} = latent heat of vaporization, $J \cdot kg^{-1}$
K = curvature, m^{-1}
k = thermal conductivity, $W \cdot m^{-1} \cdot K^{-1}$
L = length of capillary, m
M = molecular weight, $kg \cdot mol^{-1}$
P = pressure, $N \cdot m^{-2}$
Q = heat transferred in interline region, $W \cdot m^{-1}$
q = heat flux, $W \cdot m^{-2}$
$\mathfrak{R}$ = universal gas constant, $J \cdot mol^{-1} \cdot K^{-1}$
R = radius of capillary, m
S = solid thickness, m
T = temperature, K
U = overall heat-transfer coefficient, $W \cdot m^{-2} \cdot K^{-1}$
u = velocity, $m \cdot s^{-1}$
V = molar volume, $m^3 \cdot mol^{-1}$
X = length of interline region, m
x = distance, m
$\bar{\gamma}$ = dimensionless heat-transfer coefficient
γ = interfacial free energy, $J \cdot m^{-2}$
δ = film thickness, m
ϵ = percent decrease in maximum available capillary pressure and capillary heat sink
η = dimensionless film thickness
θ = contact angle, deg
ν = kinematic viscosity, $m^2 \cdot s^{-1}$
ξ = dimensionless film length coordinate

Subscripts

b = base of meniscus
E = evaporating
e = effective
fg = fluid to vapor
ℓv = liquid-vapor interface
NE = nonevaporating
s = solid
t = total
o = evaluated at interline
v = vapor phase

Superscripts

$-$ = averaged
id = ideal
r = real

Presented as Paper 78-403 at the 3rd International Heat Pipe Conference, Palo Alto, Calif., May 22-24, 1978; submitted June 14, 1978; revision received Feb. 9, 1979.

Index categories: Heat Pipes; Thermal Modeling and Analysis.

*Professor of Chemical Engineering, Dept. of Chemical and Environmental Engineering. Member AIAA.

Introduction

IN the analysis of heat pipes, it has been common practice to use a dimensional liquid transport number, $N = \gamma h_{fg}/\nu$, to evaluate the relative heat sink capability of the evaporating meniscus. In addition, the understanding of the evaporating meniscus can be enhanced by defining a "meniscus shape factor," $R(K_E^{id} - K_{NE}^{id})$, which is the product of the radius of the capillary and the change in average curvature at the base of the evaporating meniscus.[1] This shape factor is a measure of the pressure drop in the capillary resulting from the flow of fluid to the base of the meniscus, which is due to a change in the meniscus shape at its base. Although these two groups aid our understanding of the evaporating meniscus, they do not describe the effect of transport processes occurring in the interline region (thin film region at the junction of the solid, the evaporating meniscus, and the vapor) on the curvature at the base of the meniscus. That is, while the ideal maximum curvature at the base of a meniscus in a capillary with an intrinsic contact angle equal to zero is $K^{id} = 2R^{-1}$, the real maximum curvature at the base of an evaporating meniscus with an intrinsic contact angle equal to zero is less, $K_E^r = 2R^{-1}\cos\theta_e$. Herein, we use the effective or apparent contact angle, θ_e, as a measure of the viscous losses in the interline region. The analysis presented below is for a mathematically smooth surface. Therefore, the change in the value of the apparent contact angle from its intrinsic value will be due to viscous effects only and does not include a roughness effect.[2] Surface finish would have an additional effect. The intrinsic contact angle is, of course, a function of only the chemical composition at a given temperature and pressure. The effect of shear stresses in the interline region on the meniscus profile and capillary pressure are analyzed using the concepts K_E^r and θ_e. These concepts are convenient measures of the effect of microscopic transport processes in the interline region on the heat sink capability of the evaporating meniscus.

For the purpose of analysis, the extended meniscus can be divided into three zones: 1) the immediate vicinity of the interline (the thin film region), where the thickness of the liquid can vary from a monolayer to approximately 500 Å and where the fluid flow results from the varying force of attraction between the liquid and solid; 2) the inner intrinsic meniscus region, where the thickness range is approximately $0.05\text{-}10 \times 10^{-6}$ m and where fluid flow resulting from very large pressure gradients due to meniscus shape is possible; and 3) the outer intrinsic meniscus region, where the thickness is

greater than 10^{-5} m and where fluid flow resulting from small pressure gradients due to curvature is possible. The curvature of the outer intrinsic meniscus becomes a constant as the centerline of the capillary is approached.

The analysis of the evaporating meniscus recently has been extended to the interline region by evaluating the effect of the London-van der Waals dispersion force between the solid and liquid on the pressure in the liquid and on the vapor pressure of the liquid.[3,4] This analysis is based on the premise that the interline transport processes are ultimately controlled by the dispersion force resulting from the fluctuating electromagnetic fields of the solid and liquid. This effect becomes important when the thickness of the liquid is less than 10^{-7} m. Since this region is relatively short in extent, it may account for approximately 10% of the evaporation process, depending on the radius of capillary. However, since this is the location where the meniscus "hangs on to the solid," the stability of the meniscus is probably determined in this region. In addition, the contact angle and/or apparent contact angle fixes the extent of the meniscus and the capillary pressure; therefore, the region is of critical importance. In order to quantify the effect of the liquid-solid system properties on the interline heat-transfer coefficient, a solution for a constant heat flux model of the interline region has been obtained.[6] This solution demonstrates the importance of the group of properties $\bar{A}h_{fg}/\nu$, which we call the interline heat flow number and which has dimensions of watts. This replaces the dimensional liquid transport number, $\gamma h_{fg}/\nu$, as the important transport group in the interline region where the dispersion constant $\bar{A}$ is more important than the surface tension γ. Herein, we are concerned with using these models to evaluate the effect of heat transfer on the meniscus profile, the effective contact angle, and the capillary pressure.

Analysis

The following general assumptions are used in the models and definitions presented herein: 1) the solid surface is smooth; 2) fluid flow can be represented by a steady-state Newtonian continuum model; 3) the inertia terms are negligible; 4) the solid and fluid properties are constant; 5) the pressure gradient for fluid flow results from only the gradient of the pressure difference at the liquid-vapor interface; 6) the evaporative heat flux at the liquid-vapor interface is a constant in the region analyzed, $1<\eta<\eta_1$; and 7) quasiequilibrium thermodynamics can be used to describe evaporation.

The pressure difference across the liquid-vapor interface for a uniformly spherical meniscus at the exit of a capillary is given by

$$(\Delta P)_{lv} = 2\gamma\cos\theta_e/R = \gamma K \tag{1}$$

where K is defined as the total curvature of a spherical meniscus and θ_e is the apparent contact angle that the fluid makes with the *inside* wall of the capillary. Microscopically, the interline with a constant real contact angle (but varying apparent contact angle) can move around the edge of the capillary, which is not a perfect junction of two smooth surfaces. Assuming that fluid flow in a capillary tube to the base of an evaporating meniscus results from a change in the curvature at the base of the meniscus from its nonevaporating value, the pressure drop for fluid flow is given by

$$\Delta P = \gamma(K_E^{id} - K_{NE}^{id}) = \gamma K_E^{id} \tag{2}$$

in which $K_{NE}^{id} = 0$ is used herein as a base value for the purpose of analysis. This assumption places the reference "meniscus," which is flat, at the exit of a capillary tube. A small increase in the pressure inside the liquid would cause the tube to overflow; a small decrease would lead to an increase in meniscus curvature. It would, of course, be possible to use a different reference curvature for the analysis, since we are seeking the change from the reference value which is due to evaporation. Photographs of the profile of the junction of a meniscus with a corner which depicts this phenomenon recently have been published.[5] The total ideal heat flux (based on the cross-sectional area of the capillary) needed to evaporate all the fluid flowing as a result of this ideal pressure difference is:

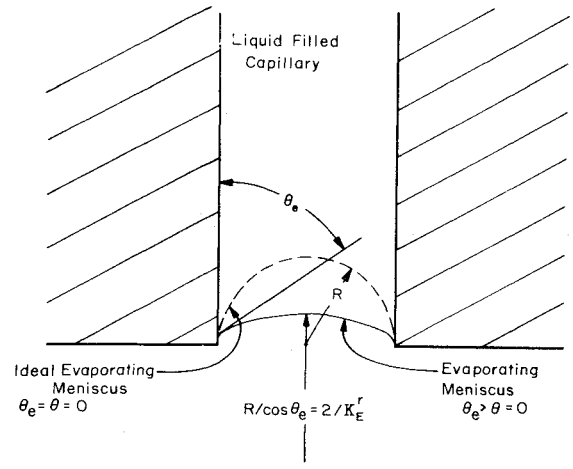

Fig. 1 Evaporating meniscus profile.

$$q_l^{id} = h_{fg}R^2\gamma K_E^{id}/8\nu L \tag{3}$$

Since viscous effects in the evaporating meniscus region cause the total real heat flux q_l^r to be less than its ideal value, we define a percent decrease in heat flux ϵ:

$$\epsilon = 100[(q_l^{id} - q_l^r)/q_l^{id}] \tag{4}$$

Using Eqs. (3) and (4) gives

$$\epsilon = 100[1 - (K_E^r/K_E^{id})] \tag{5}$$

where ϵ is a measure of both the change in maximum available capillary pressure and the change in maximum available capillary heat sink. Defining an effective contact angle, as depicted in Fig. (1), as

$$K_E^r = 2\cos\theta_e/R \tag{6}$$

and using $K_E^{id} = 2/R$ with $\theta = 0$ for the ideal case, we obtain

$$\epsilon = 100[1 - \cos\theta_e] \tag{7}$$

The effective contact angle is a measure of the remaining suction potential if we assume, for the purpose of analysis, that the rest of the meniscus beyond the point of measuring θ_e is spherical. For the current analysis, we are evaluating only the effect of viscous losses in the immediate viscinity of the interline defined as the dimensionless thickness range $1<\eta<\eta_1$. Since the apparent contact angle increases faster in the real case due to viscous losses, a measurable decrease in capillary pressure is observed. The contact angle in terms of the slop of the interface at $\eta = \eta_1$ is:

$$\theta_e|_{\eta_1} = \tan^{-1}(d\delta/dx)_{\eta_1} \tag{8}$$

It is well known that the vapor pressure over an adsorbed film of a nonpolar liquid is a function of the temperature and the London-van der Waals dispersion force of attraction between the solid and liquid (e.g., Refs. 3 and 4 are of particular relevance). This fact can be used to predict the effect of the evaporative heat flux in the interline region on the meniscus profile and, therefore, ϵ. The interline heat-transfer coefficient and the interline heat sink capability can also be

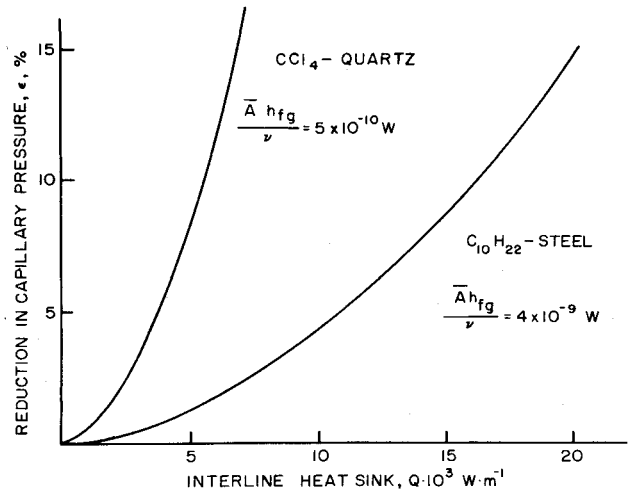

Fig. 2 Theoretical percent reduction in maximum available capillary pressure or in maximum available heat sink ϵ vs interline heat sink Q for $\bar{\gamma}=0.5$ and $\eta=10$.

obtained as a function of the interline heat flow number $\bar{A}h_{fg}/\nu$ in which $\bar{A}$ is a dispersion constant accounting for the attractive force between the liquid and solid, h_{fg} is the heat of vaporization, and ν is the kinematic viscosity.[6] For example, a constant heat flux model of the evaporating interline region[6] shows that

$$\ell_n(\eta)=\bar{\gamma}\xi^2/2 \tag{9}$$

in which $\eta=\delta/\delta_0$, $\bar{\gamma}=\bar{q}/q^{id}$ (note: $q^{id}\neq q_l^{id}$), and $\xi^2=Gx^2$. δ_0 is the thickness of the thin film at the interline, q^{id} is the local ideal heat flux based on the kinetic theory of vapor flow, and $\bar{q}$ is the average heat flux in the thin film region of interest $\eta>1$. The length is made dimensionless using[7]

$$G=\frac{2\nu}{\bar{A}}\left(\frac{M}{2\pi\Re\bar{T}}\right)^{1/2}\left(\frac{p_vMh_{fg}}{\Re}\right)\left(\frac{T_{\ell v}-T_v}{T_{\ell v}T_v}\right) \tag{10}$$

Equation (9) can be differentiated to obtain the slope

$$\frac{d\delta}{dx}=(2G\bar{\gamma}\ell_n\eta)^{0.5}\delta_0\eta \tag{11}$$

Using the following two equations from Ref. 3:

$$h_{fg}\bar{A}G/\nu=q^{id} \tag{12}$$

$$Q=(2\bar{q}\ell_n\eta)^{0.5}(h_{fg}\bar{A}/\nu)^{0.5} \tag{13}$$

we obtain Eq. (14) for the slope.

$$\frac{d\delta}{dx}=\frac{Q\delta_0\nu\eta}{h_{fg}\bar{A}} \tag{14}$$

Equation (14) gives the slope at η as a function of the dimensionless interline heat sink, $Q\delta_0\nu\eta/\bar{A}h_{fg}$. Therefore, the change in slope at η on a smooth surface from its intrinsic value (zero for the systems discussed herein) is equal to a dimensionless interline heat sink. The dimensional interline heat flow number $h_{fg}\bar{A}/\nu$ is a property of the system and can be evaluated using the procedures outlined in Ref. 4. The interline thickness can be obtained using the following equation[7]:

$$\delta_0=\left(\frac{\bar{A}V_\ell T_v}{Mh_{fg}(T_{\ell v}-T_v)_0}\right)^{1/3} \tag{15}$$

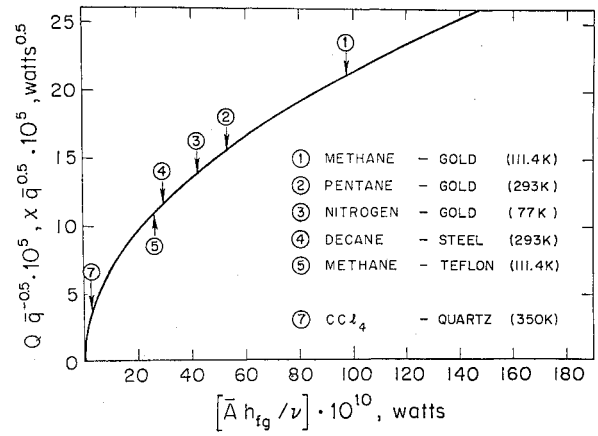

Fig. 3 Graphical representation of theoretical equations, Eqs. (13) and (17), for $\eta=10$.

Although this completely defines a procedure to evaluate the loss in heat sink capacity resulting from viscous losses in the interline region, a simple method to obtain the effect of microconduction in the solid on the local heat flux distribution has not yet been formulated. The two available models for the local heat flux, constant heat flux,[6] and constant surface temperature[7] are approximate in nature. Using the constant heat flux model, Eq. (16) is obtained by combining Eqs. (8) and (13-15):

$$\theta_e=\tan^{-1}\left\{\eta\left[(2\ell_n\eta)\left(\frac{\bar{A}V_\ell h^{id}T_v}{Mh_{fg}}\right)\left(\frac{\nu}{h_{fg}\bar{A}}\right)^2\bar{\gamma}Q\right]^{1/3}\right\}_{\eta_l} \tag{16}$$

The groups $(\bar{A}V_\ell h^{id}T_v/Mh_{fg})$ and $(\nu/h_{fg}\bar{A})$ are not strong functions of the *small* variation in the local interfacial temperature resulting from conduction. Therefore, θ_e is primarily a function of η, $\bar{\gamma}$, and Q. For the purpose of comparing two systems, η can be chosen arbitrarily. $\bar{\gamma}$ is an unkown but obtainable measure of the effect of local conduction on the microscopic scale on the interline temperature difference $(T_{\ell v}-T_v)_0$. Again, for the purpose of comparison and a qualitative understanding of the effect of viscous losses on the percent decrease in heat flux, we can set $\bar{\gamma}$. A reasonable choice is $\bar{\gamma}=0.5$.

Results

Equations (7) and (16) were used to obtain the effect of the interline heat sink Q on the percent reduction in the maximum available capillary pressure ϵ. These results are presented in Fig. 2 for C Cl_4-quartz (350 K) and $C_{10}H_{22}$-steel (447 K) systems with $\bar{\gamma}=0.5$ and $\eta=10$. The values for the interline heat flow number are from Ref. 4, wherein the dispersion constants are obtained from the optical properties of the system. The percent reduction in capillary pressure is much greater for the C Cl_4-quartz system. This is primarily due to the effect of the dimensional interline heat flow number, $h_{fg}\bar{A}/\nu$, on the interline heat sink Q as given by Eq. (13). For these two cases, the change in the value of $h_{fg}\bar{A}/\nu$ is primarily due to the change in the value of the dispersion constant $\bar{A}$, which is a measure of the London-van der Waals force of attraction between the solid and the liquid. A discussion of the effect of $\bar{A}$ on heat transfer is given in Ref. 7. Briefly, this force is electromagnetic in origin and arises from the second-order perturbation theory applied to the electrostatic interaction between dipoles.[8,9] An increase in the interline heat flow number gives an increase in Q for the same values of $\bar{q}$ and η. This, in turn, is a result of the increase in the length of the interline region of thickness range $\eta>1$, X, which is a function of the interline heat flow number[4]:

$$X=(2\ell_n\eta)^{0.5}(\bar{q})^{-0.5}(h_{fg}\bar{A}/\nu)^{0.5} \tag{17}$$

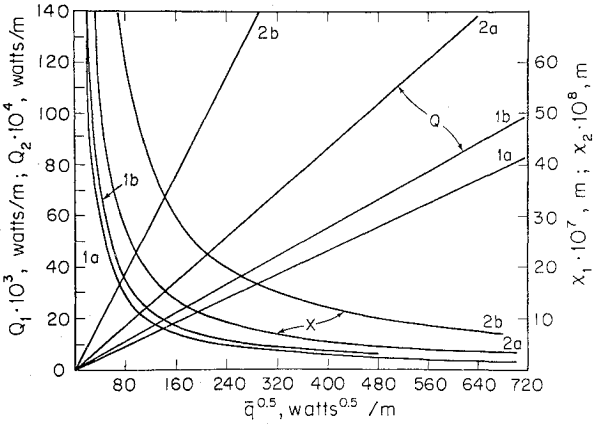

Fig. 4 Theoretical heat sink capability Q and theoretical interline length x for $\eta = 10$: 1a) decane-steel at 293 K; 1b) decane-steel at 447 K; 2a) CCl_4-quartz at 293 K; 2b) CCl_4-quartz at 350 K.

Equations (13) and (17) are presented in Figs. 3 and 4 for $\eta = 10$. In Fig. 3 some of the values of $\bar{A}h_{fg}/\nu$ for various systems are marked on the theoretical curve. Obviously, an increase in the interline heat flow number gives an increase in the theoretical heat sink Q and the length of the interline region x. Two of the systems, decane-steel and carbon tetrachloride-quartz, are given in more detail in Fig. 4. Curve 1 represents the carbon tetrachloride-quartz system at 293 and 350 K. The results predict that the interline heat sink Q for the decane-steel system is approximately three times larger than that for the carbon tetrachloride-quartz system at the same heat flux and $P_v = 1.01 \times 10^5 \text{N} \cdot \text{m}^{-2}$. This results from the increased length of the evaporating thin film x of thickness $1 < \eta \leq 10$, which is a function of the interline heat flow number. The increase of Q with temperature results from the substantial decrease in the kinematic viscosity in this temperature range. This increase will not continue since the dispersion constant will decrease substantially at higher temperatures. For the carbon tetrachloride-quartz system, both the dispersion constant and the reciprocal of the kinematic viscosity increase with temperature at this temperature level.

For a more extensive numerical example, we compare the heat-transfer characteristics of an evaporating thin film of carbon tetrachloride on quartz with those of decane on steel in Table 1. The size of the ideal heat flux is approximately fixed by the vapor pressure and temperature difference for all practical purposes. Therefore, it is desirable to compare the two systems at the same vapor pressure level for which we use the atmospheric pressure of $1.01 \times 10^5 \text{N} \cdot \text{m}^{-2}$. Although this is desirable from a heat transfer point of view, it does add an additional uncertainty, since the extrapolated values of $\bar{A}h_{fg}\nu^{-1}$ are used. The interline temperature difference of 10^{-2} K is used to fix the heat flux level at approximately $\bar{q} = 16{,}000 \text{ W} \cdot \text{m}^{-2}$. Due to the larger value of $\bar{A}$, the interline thickness δ_0 and the interline length x of the decane-steel system are larger than those of the carbon tetrachloride-quartz system. This gives the decane system a higher heat sink capability Q. As presented in Ref. 6, the equation for the interline heat sink can be written as

$$Q = [2\ell n(\eta) k_s (T_s - T_v) S^{-1}]^{0.5} [\bar{A}h_{fg}\nu^{-1}]^{0.5} \tag{18}$$

thereby defining an effective overall heat-transfer coefficient U_e as

$$U_e = [2k_s \bar{A}h_{fg}/\nu S(T_s - T_v)]^{0.5} \tag{19}$$

for

$$Q = U_e [\ell n \eta]^{0.5} [T_s - T_v] \tag{20}$$

Values for U_e are also given in Table 1. The larger values of the interline heat flow number and the thermal conductivity of the solid combine to give the decane-steel system a much larger effective overall heat-transfer coefficient U_e. For comparison, the heat-transfer characteristics are also given for $T_v = 293$ K. Although it is not possible to predict the maximum stable heat flux at the present time, the larger values of $\bar{A}$ and δ_0 for the decane-steel system should also give a larger maximum stable heat flux.

Discussion

A theoretical procedure to determine the effect of the macroscopic optical properties and the thermophysical properties of the system on the reduction in capillary pressure has been outlined. This procedure significantly increases our understanding of the interline and shows how the level of interline transport processes affect the maximum available capillary pressure. Due to the basic nature of the equations, their current level of development, and the limited availability of data, the use of ideal systems (e.g., neglecting surface roughness) has been emphasized. However, this does not detract from the significance of the results, since ideal systems give an order-of-magnitude approximation and enhanced understanding of real systems, and reveal the basic mechanisms involved in the transport processes.

Experimental studies were conducted on the meniscus region where the film thickness δ was greater than 1020 Å.[1,10,11] This paper predicts the effects occurring in the region $\delta < 1200$ Å. The experimental results given in Refs. 10 and 11

Table 1 Theoretical comparison of carbon tetrachloride-quartz system with the decane-steel system

$T_v = 293$ K	CCl_4-quartz, $T_v = 293$ K	$C_{10}H_{22}$-steel, $T_v = 293$ K	$C_{10}H_{22}$-steel $T = 447.2$ K	CCl_4-quartz, $T_v = 349.7$ K
$\delta_0 \cdot 10^{10}$, m	29	103	121	45
$G \cdot 10^{-10}$, m^{-2}	7000	6.4	800	6560
$h_{fv}^{id} \cdot 10^{-4}$, W·m^{-2}·K^{-1}	74	1.85	330	326
$\bar{A} \cdot 10^{22}$, N·m	3[a]	100[a]	66	7.7
$(h_{fg}\bar{A}/\nu) \cdot 10^{10}$, W	1.05	29	41.4	4.97
$P_v \cdot 10^{-4}$, N·m^{-2}	1.19	0.012	10.1	10.1
$\bar{q}^{id} \cdot 10^{-4}$, W·m^{-2}	0.74	0.0186	3.3	3.26
$\bar{q} \cdot 10^{-4}$, W·m^{-2}	0.37	0.0093	1.65	1.63
γ	0.5	0.5	0.5	0.5
η	10	10	10	10
$Q \cdot 10^3$, W·m^{-1}	1.34	1.12	17.5	6.19
$x \cdot 10^6$, m	0.36	12	1.05	0.38
$U_{\text{eff}} \cdot 10^4$, W·m^{-1}·K^{-1}	3.10	2040	179.8	3.17
S, m	10^{-3}	10^{-3}	10^{-3}	10^{-3}
$(T_s - T_v)$ K	≈ 2.85	≈ 0.0036	≈ 0.65	≈ 12.7
$(T_{fv} - T_v)_0$, K	0.01	0.01	0.01	0.01

[a] Experimental values.

show that the apparant contact angle is a function of heat flux. The intrinsic contact angle was taken to be a constant in these references. Therefore, our previous experiments on the region $\delta > 1200$ Å support the general conclusions of this study. However, they did not have sufficient detail in the region $\delta < 1200$ Å to evaluate our new models. These results will be useful in designing a new set of experiments specifically for determining the effect of interline transport processes on the meniscus profile and capillary pressure.

Conclusions

1) Viscous flow of the evaporating liquid in the interline region of the meniscus has a significant effect on the effective contact angle of the meniscus. For large heat fluxes, the increase in the effective contact angle can be of the order of 30 deg.

2) The capillary pressure of the meniscus is significantly reduced as a result of an increase in the effective contact angle with heat flux. For large heat fluxes, this decrease can be of the order of 15%.

3) The interline heat sink capability of a simple fluid on metal is greater than that of a simple fluid on glass because the London-van der Waals dispersion force in the metal-fluid system is greater than that in the glass-fluid system.

4) The dispersion model of interline heat transfer predicts measurable changes in the meniscus characteristics which depend on the macroscopic "optical" properties of the solid and liquid.

Acknowledgment

The author gratefully acknowledges the financial support of NSF Grant ENG76-01608.

References

[1] Preiss, G. and Wayner, P. C., Jr., "Evaporation from a Capillary Tube," *Journal of Heat Transfer, Transactions of ASME*, Series C, Vol. 98, May 1976, pp. 178-181.

[2] Adamson, A. W., *Physical Chemistry of Surfaces*, 2nd ed., Interscience Publishers, New York, 1967, p. 358.

[3] Potash, M. L., Jr. and Wayner, P. C., Jr., "Evaporation from a Two Dimensional Extended Meniscus," *International Journal of Heat and Mass Transfer*, Vol.15, Oct. 1972, pp. 1851-1863.

[4] Wayner, P. C., Jr., "The Effect of the London-van der Waals Dispersion Force on Interline Heat Tranfer," *Journal of Heat Transfer, Transactions of ASME*, Vol. 100, Feb. 1978, pp. 155-159.

[5] Bayramli, E. and Mason, S. G., "Liquid Spreading: Edge Effect of Zero Contact Angle," *Journal of Colloid and Interface Science*, Vol. 66, Aug. 1978, pp. 200-202.

[6] Wayner, P. C., Jr., "A Constant Heat Flux Model of the Evporating Interline Region," *International Journal of Heat and Mass Transfer*, Vol. 21, March 1978, pp. 362-364.

[7] Wayner, P. C., Jr., Kao, Y. K., and Lacroix, L. V., "The Interline Heat Transfer Coefficient of an Evaporating Wetting Film," *International Journal of Heat and Mass Transfer*, Vol. 19, May 1976, pp. 487-492.

[8] Chu, B., *Molecular Forces, Based on the Baker Lecturers of Peter J. W. Debye,* Interscience Publishers, New York, 1967.

[9] Dzyaloshinskii, I. E., Lifshitz, E. M., and Pitaevskii, L. P., "The General Theory of van der Waals Forces," *Advances in Physics*, Vol. 10, 1959, pp. 165-209.

[10] Renk, F. and Wayner, P. C., Jr., "The Measurement of Fluid Flow and Heat Transfer in an Evaporating Meniscus," *Proceedings of the Fifth International Heat Transfer Conference*, Tokyo, Japan, Vol. 5, 1974, pp. 252-256.

[11] Renk, F. J. and Wayner, P. C., Jr., "An Evaporating Ethanol Meniscus, Part I, Experimental Studies," *Journal of Heat Transfer, Transactions of ASME*, Vol. 101, Feb. 1979, pp. 55-58.